This article was downloaded by: [University of California, San Diego]
On: 20 August 2012, At: 22:15
Publisher: Taylor & Francis
Informa Ltd Registered in England and Wales Registered Number: 1072954 Registered office: Mortimer House, 37-41 Mortimer Street, London W1T 3JH, UK

Molecular Crystals and Liquid Crystals Science and Technology. Section A. Molecular Crystals and Liquid Crystals

Publication details, including instructions for authors and subscription information:
http://www.tandfonline.com/loi/gmcl19

Atomic Force Microscopy and Grazing Incidence Diffraction Investigation of the Gas-Solid Diazotation of Sulfanilic Acid

Andreas Herrmann [a] , Gerd Kaupp [a] , Thomas Geue [b] & Ulrich Pietsch [b]

[a] Universität Oldenburg, Fachbereich Chemie, Postfach 2503, D-26111, Oldenburg

[b] Universität Potsdam, Institut f. Festkörperphysik, Am neuen Palais 10, D-14469, Potsdam

Version of record first published: 04 Oct 2006

To cite this article: Andreas Herrmann, Gerd Kaupp, Thomas Geue & Ulrich Pietsch (1997): Atomic Force Microscopy and Grazing Incidence Diffraction Investigation of the Gas-Solid Diazotation of Sulfanilic Acid, Molecular Crystals and Liquid Crystals Science and Technology. Section A. Molecular Crystals and Liquid Crystals, 293:1, 261-275

To link to this article: http://dx.doi.org/10.1080/10587259708042776

PLEASE SCROLL DOWN FOR ARTICLE

Full terms and conditions of use: http://www.tandfonline.com/page/terms-and-conditions

This article may be used for research, teaching, and private study purposes. Any substantial or systematic reproduction, redistribution, reselling, loan, sub-licensing, systematic supply, or distribution in any form to anyone is expressly forbidden.

The publisher does not give any warranty express or implied or make any representation that the contents will be complete or accurate or up to date. The accuracy of any instructions, formulae, and drug doses should be independently verified with primary sources. The publisher shall not be liable for any loss, actions,

claims, proceedings, demand, or costs or damages whatsoever or howsoever caused arising directly or indirectly in connection with or arising out of the use of this material.

Downloaded by [University of California, San Diego] at 22:15 20 August 2012

Mol. Cryst. Liq. Cryst., 1997, Vol. 293, pp. 261–275
Reprints available directly from the publisher
Photocopying permitted by license only

© 1997 OPA (Overseas Publishers Association)
Amsterdam B.V. Published in The Netherlands under
license by Gordon and Breach Science Publishers
Printed in Malaysia

Downloaded by [University of California, San Diego] at 22:15 20 August 2012

Atomic Force Microscopy and Grazing Incidence Diffraction Investigation of the Gas-Solid Diazotation of Sulfanilic Acid

ANDREAS HERRMANN[a], GERD KAUPP[a], THOMAS GEUE[b] and ULRICH PIETSCH[b]

[a]*Universität Oldenburg, Fachbereich Chemie, Postfach 2503, D-26111 Oldenburg;*
[b]*Universität Potsdam, Institut f. Festkörperphysik, Am neuen Palais 10, D-14469 Potsdam*

(Received 16 June 1996)

The solid state diazotation of sulfanilic acid monohydrate (I) on (010) gives island features and craters on the surface. The remaining surface roughness stays low enough to permit depth dependent grazing incidence X-ray diffraction (GID) measurements, but only when the gas applications are slow. The theoretical background of the unprecedented GID measurements is given. GID measurements were undertaken below, at and above the critical angle of incidence to differentiate the processes at the surface and in the crystal bulk. The phase rebuilding and phase transformation processes could be directly detected in the bulk of the crystal supporting the common AFM interpretations which are derived from the formation of surface features in correlation with crystal packing data. The combined consideration of depth resolved in-plane GID and AFM experiments leads to a comprehensive description of the gas-solid process.

Keywords: AFM; GID; synchrotron; sulfanilic acid; diazotation; phase rebuilding; depth dependent diffraction

INTRODUCTION

Atomic Force Microscopy (AFM) provides new answers for organic solid-state reactivity. New and unexpected details are unraveled which cannot be obtained by any other technique, presently. The new concept of phase rebuilding enables comprehension of the necessity for far-reaching anisotropic molecular movements on the basis of crystal structure data. That requirement

for reactivity was not foreseen and not considered to be existing [1]. AFM is a local technique that images surface topography. The phenomenological description of the phase rebuilding during chemical reaction must be interpreted with respect to known crystal packing properties. However, direct information about the processes in the crystal bulk require additional techniques such as grazing incidence X-ray diffraction (GID) with synchrotron sources. The angle of incidence α_i can be kept below the critical angle of total reflection α_c. The penetration depth of the X-ray beam L_i is limited to about 5 nm for that condition. If however, α_i is chosen larger than α_c, the penetration depth increases discontinuously and information from the crystal bulk is obtained. By systematic variation of α_i depth dependent diffraction profiles (α_f-profiles) are obtained. These are used here for the investigation of the diazotation of single crystals of sulfanilic acid monohydrate with gaseous NO_2.

GAS-SOLID DIAZOTATIONS WITH NITROGEN DIOXIDE

Nitrogen dioxide is an ubiquitous toxic gas from (automotive) firings which poses severe problems to the atmospheric environment. It is a free radical and has a high reactivity which allows elegant applications in numerous gas-solid syntheses which, unlike common solution reactions, proceed quantitatively and avoid wastes [2,3]. An important example is the diazotation of sulfanilic acid (**1**) to give its diazonium salt (**3**), which is needed for the synthesis of the well known indicator methylorange (via azo coupling with *N,N*-dimethylaniline).

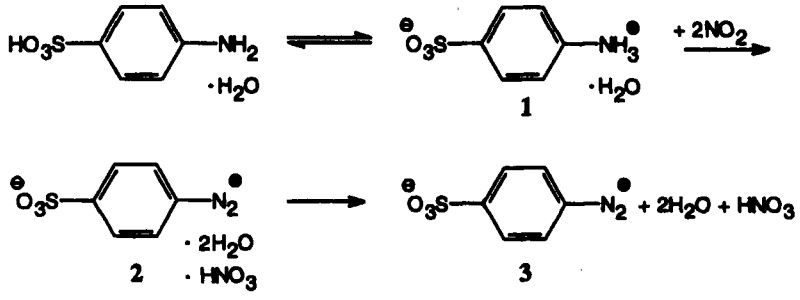

Both anhydrous sulfanilic acid or its monohydrate, which forms monoclinic prisms with 1–3 mm long edges, diazotize quantitatively under the action of gaseous NO_2. The solid product crystals may be safely ground in an agate mortar (avoiding all kinds of sharp edges). They are, however, as

Downloaded by [University of California, San Diego] at 22:15 20 August 2012

are other solid diazoniums salts, explosive if heavily hit on an anvil. The crystal data of **1** ($P2_1/c$, $a=6.473$, $b=18.308$, $c=6.812$ Å, $\beta=93.63°$) [4] and **3** ($P2_1/c$, $a=8.02$, $b=9.81$, $c=11.46$ Å, $\beta=126.7°$) [5] are known. The structure of **2** is unknown.

AFM INVESTIGATIONS

The AFM results help in search, systematization and prediction of further waste-free solid state reactions. That is achieved by direct indication of the reasons for the success of these new synthetic techniques. All kinds of waste-free solid-state syntheses without solvent will undoubtedly turn out to be the production techniques of the future. Photoreactions of crystals have been used extensively [1], however, their large-scale technical use poses difficulties. More profitable appear gas-solid [6] and solid-solid [7] syntheses. These were severely hampered by incomplete theories of topochemistry [8] that did not cover all reactivity factors and thus could not "explain" gas-solid and solid-solid reactivity. That situation has now changed by the new theoretical foundation [1, 6, 9]. The AFM investigation on the (010) pinacoid of sulfanilic acid monohydrate at a rather massive application of NO_2 is shown in Figure 1. The starting surface (Fig. 1a) shows traces of their well-known efflorescence in the form of tiny volcanoes. These features disappear after the first application of NO_2 in air. Flat islands which tend to include little craters are formed (Fig. 1b, d). The characteristic island features are still recognizable after multiple application of NO_2 (Fig. 1c). However, the advanced height growth is remarkably slow and less uniform. A more roughened height scenery with embraced craters is obtained. The formation of islands [10] is a consequence of the crystal structure of sulfanilic acid monohydrate [4], which is depicted in Figure 2. The hydrogen bridged molecules stand vertically on their narrow side under (010) and their orientation alternates. The water molecules add further hydrogen bridging. While the upmost layer on (010) has half of the molecules with their NH_2-groups freely accessible to attack by NO_2 to give diazotation (Fig. 2, top), any proceeding of the reaction under (010) would require that the long elongated molecules exit from their H-bonded lattice positions and move upward in order to make all amino groups available for diazotation which either pointed downward in the first layer or upward in the second layer etc. Clearly such reaction is hindered by the particular packing in Figure 2. Therefore the reaction tends to spread around the initially successful invasions. The island formation [10] proceeds so orderly, that two parallel

Downloaded by [University of California, San Diego] at 22:15 20 August 2012

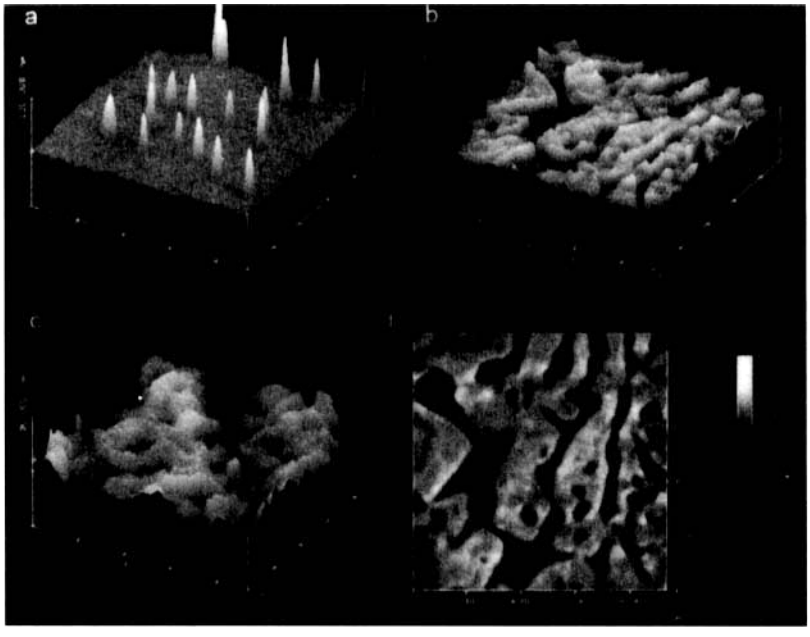

FIGURE 1 AFM topography of the (010) surface of sulfanilic acid monohydrate; (a): fresh and hardly effloresced; (b)/(d): island formation after 1 min diazotation with 2 ml of 70% NO_2 gas as applied from 1 cm distance; (c): after 6 treatments with 2 ml of 70% NO_2 gas each.

levels at a distance of 15 nm are initially formed on the surface (Fig. 1b, d). Subsequently the AFM images hardly change upon further addition of NO_2. Nevertheless, the reaction proceeds, but that is only seen after massive application of NO_2 (Fig. 1c, after 6 fold application of NO_2). It appears, that the NO_2 molecules have to attack at crystal defects, e.g. from the sides of the infinite chains at the slopes of the craters. Such reaction would be virtually unhindered, provided that the volume of the crystal does not increase significantly. Despite the good parallelism of the island surfaces with the lower plane, the features in Figure 1b are by far too high for GID measurements. As the craters within the islands (Fig. 1) and the crystal packing (Fig. 2) suggested a mechanism similar to the diazotation of anthranilic acid (where the side face of the crystal could be probed with the AFM) [11], it could be assumed that after initial diazotation of all freely accessible NH_2-groups at the surface the bulk reaction proceeds primarily from the sides of the hydrogen bonded chains. These should be accessible from crystal faults such as the developing crater faces. We decreased the height of the islands and favoured the formation of the craters by slowing

Downloaded by [University of California, San Diego] at 22:15 20 August 2012

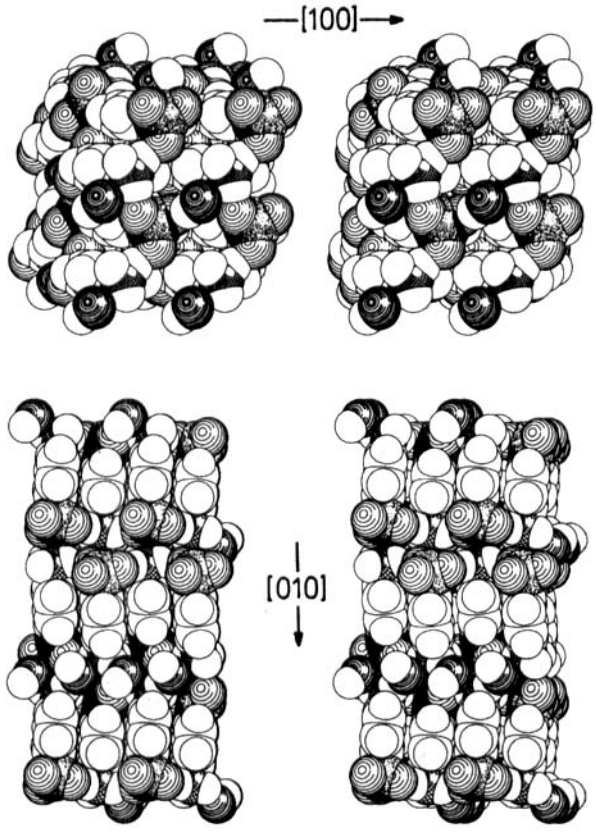

FIGURE 2 Stereoscopic representation of the molecular packing of sulfanilic acid monohydrate; top: view on the (010)-face showing hydrogen bridges between ammonium and sulphonate-groups with additional hydrogen bridging by H_2O molecules; bottom: view on (100) which is orthogonal to (010), showing that the molecules alternate in their orientation and that they stand vertically under the (010)-face which is on top; N: grid; S: shaded; O at S: circles; O of water molecules: dense circles.

down the reaction rate. Thus, at a 10 times slower application of NO_2 the height of the islands decreased to the 1 nm scale which was tolerable for the GID experiment. That feature is clearly illustrated in Figure 3. It shows that the initial roughness is flattened out after the first application of the reactant gas. Thus, the very efficient diazotation reacts all freely accessible amino groups at the surface and levels it. 3 further additions give rise to 1–1.8 nm high large area islands (Fig. 3c). After the fifth and sixth addition of NO_2 numerous craters are seen (Fig. 3d). Further additions do not significantly change the surface any more. It is to be expected that any further progress of the reaction

Downloaded by [University of California, San Diego] at 22:15 20 August 2012

starts at the crater slopes which stand steeply under the (010) face of **1** and works itself laterally and vertically into the crystal bulk well under the surface. This mechanism was largely impeded in Figure 1 due to the 10 times higher concentration of NO_2. While the natural side-faces of our single crystals of **1** were too small for the AFM measurements, it was possible to prove that mechanism by GID measurements under the roughness conditions of Figure 3.

GRAZING INCIDENCE DIFFRACTION MEASUREMENTS (GID)

Several GID-investigations were carried out at surfaces to monitor dynamic phenomena such as melting of ice [12], of Cu_3Au [13] and of semiconductor surfaces [14]. However, the application of GID-techniques to organic gas-solid reactions is unprecedented.

The GID experiments were carried out at the triple-axis diffractometer D4.1 at Hasylab (Hamburg, Germany). The wavelength was set to $\lambda = 1.48$ Å.

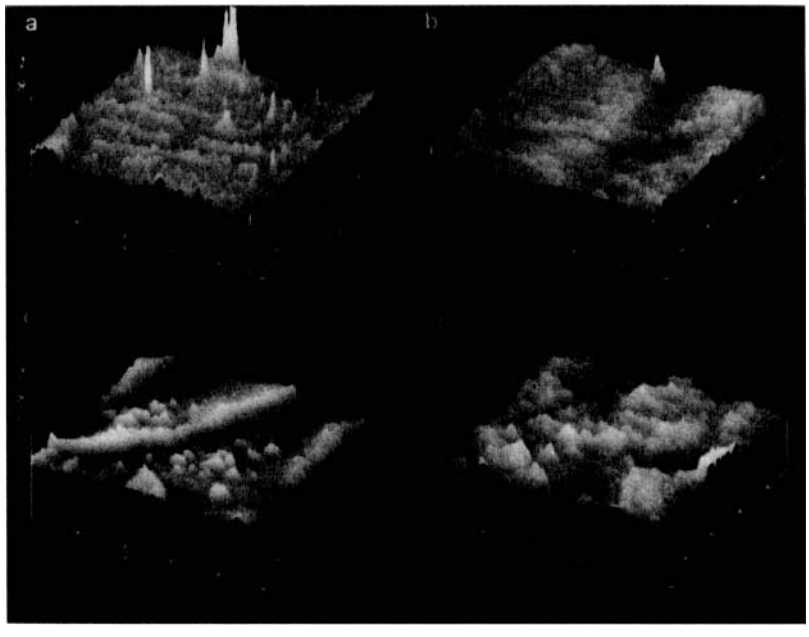

FIGURE 3 AFM surfaces of **1** on (010); (a) fresh; (b) after application of 1 ml 15% NO_2 in air from 1 cm for 1 min; (c) after similar application of 4 portions 15% NO_2; (d) after 6 portions of NO_2.

Downloaded by [University of California, San Diego] at 22:15 20 August 2012

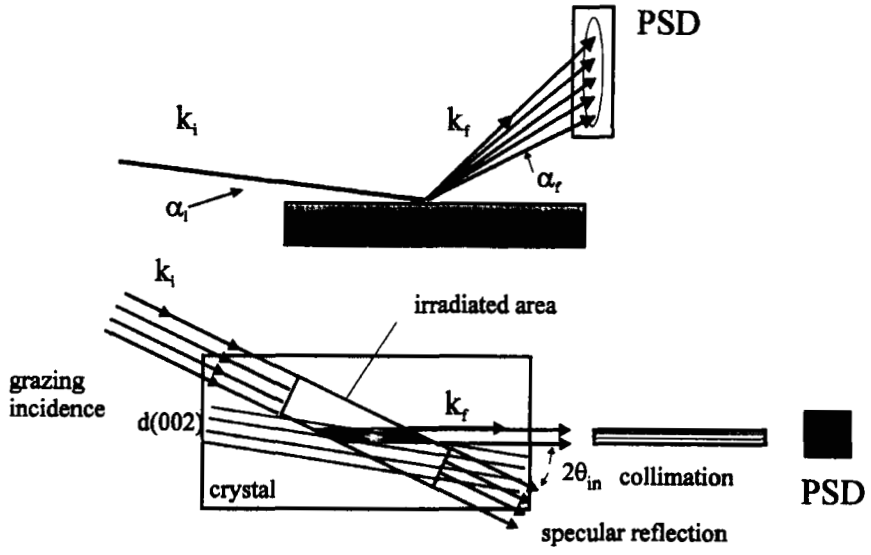

FIGURE 4 Side and top view of the diffraction geometry at grazing incidence; only the shaded part of the crystal contributes to the diffracted intensity; the position sensitive detector (PSD) is vertically mounted.

The experimental setup is schematically shown in Figure 4. A position sensitive detector (PSD) was used to measure the angular position $2\theta_{in}$ of the in-plane diffraction signals as well as the intensity distribution as a function of the exit angle α_f (rod scans) simultaneously. The resolution along α_f amounted to 0.0055°. The collimation of the incoming monochromatic synchrotron beam was better than $\Delta\alpha_i \approx 0.005°$ and $\Delta\theta_{in} \approx 0.01°$. The (002)-reflection of the monoclinic sample (1×0.5 mm^2 area) was chosen for the measurements owing to the perpendicular arrangement of the net plane relative to the surface normal.

The well collimated highly parallel synchrotron beam strikes the sample surface under an angle of incidence α_i. The $2\theta_{in}$-angle was fixed close to the calculated BRAGG-position (values from [4]) for the (002)-reflection. The sample was then rotated around the surface normal (ω-scan) to detect the appropriate angular position in which ω fulfills the BRAGG-condition. The appearance of a surface BRAGG reflection was proven via an α_i-scan where the α_f-integrated signal was recorded as a function of α_i. This procedure provides the critical angle of total external reflection α_c where the integrated intensity becomes maximum. For fixed α_i the intensity distribution measured as a function of the exit angle α_f

Downloaded by [University of California, San Diego] at 22:15 20 August 2012

(crystal truncation rod, CTR) is calculated by

$$I(\alpha_f) \approx |S(q_z)\, T(\alpha_i)\, T(\alpha_f)|^2 \tag{1}$$

where $T(\alpha_i)$ and $T(\alpha_f)$ are FRESNELS transmission functions, becoming maximal at values of $\alpha_{i,f} = \alpha_c$ and approaching towards 1 for $\alpha_{i,f} > \alpha_c$.

Therefore a CTR displays primarily the function $|T(\alpha_f)|^2$. It is overlapped by the CTR-scattering function $S(q_z)$, which varies as a function of momentum transfer

$$q_z = 2\pi/\lambda[(\alpha_i^2 - \alpha_c^2)^{1/2} + (\alpha_f^2 - \alpha_c^2)^{1/2}] \tag{2}$$

perpendicular of the surface. In kinematic approach $S(q)$ is determined by

$$S(q_z) \approx F(hkl)|^2\, \delta(q\| - G(hkl))\; 1/[1\text{-}\exp(i\, q_z\, a)|^2 \tag{3}[15]$$

$F(hkl)$ is the structure factor of the respective BRAGG-reflection expressed by its Miller indices h, k, l of a net plane which is arranged perpendicularly to the surface. $S(q_z)$ becomes maximum also at $\alpha_{i,f} = \alpha_c$, owing to the complex character of q_z. Only if $q\|$ equals the reciprocal lattice vector $G(hkl)$, $S(q_z)$ is independent from $q\|$. This was taken into account using the KRONECKER δ in eq. (3). Otherwise the in-plane rocking curve of the BRAGG reflection is projected towards α_f following the relation $2\sin\Delta\theta_{in}$ $\Delta\theta_{in} = (\alpha_f^2 - \alpha_i^2)$ [16–18]. This effect occurs even if $\Delta\theta_{in}$ is in the range of a few seconds of arc being typical for perfect single crystals.

The grazing incidence diffraction allows a depth resolution of the diffraction. This is due to the complex character of the last term in eq. (3). L_i defines the length perpendicular to the surface for which the intensity is reduced by a factor of $1/e$. This is realized by eq. (4)

$$L_i = (\mathrm{Im}\, q_z)^{-1} \tag{4}$$

neglecting the absorption q_z which is imaginary whenever $\alpha_i < \alpha_c$. In this case the incoming wave becomes evanescent, i.e. the exponentially damped wave propagates parallel to the sample surface. Their penetration depth is very small, it amounts to about 44 Å for the present investigations.

If $\alpha_i > \alpha_c$, then L_i is approximately defined by the linear photoabsorption coefficient μ and L_i varies with $L \approx \sin\alpha_i/\mu$. For weak absorbing materials as in the case described here L_i approaches some 100 nm.

Downloaded by [University of California, San Diego] at 22:15 20 August 2012

RESULTS AND DISCUSSION

Single crystalline monoclinic prisms of sulfanilic acid monohydrate **1** with an edge length of 1 and 0.5 mm were used for the investigation of the diazotation reaction. The single crystals were mounted optically parallel with respect to the incoming monochromatic synchrotron beam ($\lambda = 1.48$ Å) and a fundamental reflection was searched. Measurements were done at the in-plane (002) reflection (structure factor $F = 26.5$) [4]. The maximum of the diffracted intensity was found to be $2\theta = 24.980°$. The maximum value of ω was determined via a scan around the surface normal (Fig. 5).

The FWHM in 2θ was only 0.0078°; this value is in the range of the half widths for reflexes which are typical of single crystalline semiconductor materials [14, 17]. Thus, a high crystalline perfection of the initial state of the crystal is indicated. The half widths in ω are independent from the value of α_i, and the single crystalline order at different penetration depths L_i remains almost perfect. The critical angle α_c was found to be 0.17°. It corresponds to an electron density of about 0.44 $Å^{-3}$ which is in fairly good agreement to that indicated by the crystal data [4]. The depth dependent diffraction profiles at the (002) reflection of the neat sulfanilic acid monohydrate single crystal before starting the diazotation reaction are displayed in Figure 6. The PSD was mounted for all the investigations in such a position that the depth dependent scans could be obtained up to α_f values

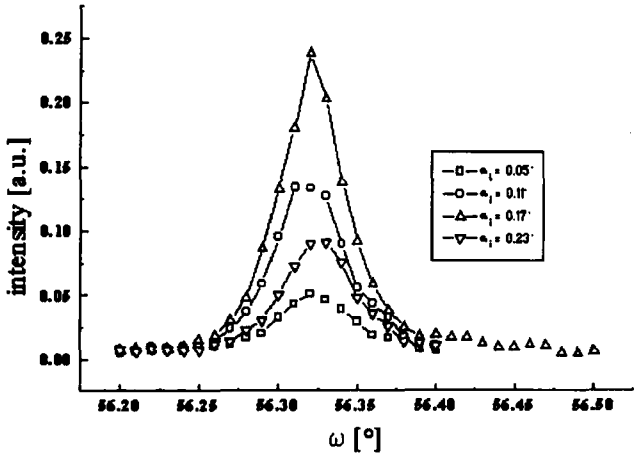

FIGURE 5 Scan around the surface normal (ω-scan) of the (002) reflection ($\lambda = 1.48$ Å, FWHM $= 0.047 \pm 0.005°$) of a single crystal of sulfanilic acid monohydrate at different angles of incidence α_i.

Downloaded by [University of California, San Diego] at 22:15 20 August 2012

of 3.41°. As expected, single maxima were observed within the monitored angular range, with the exceptions at $\alpha_i = 0.11°$ and 0.17°. The second peak at higher α_f appears to be due to the crystalline imperfections of the investigated sample (see eq. (3) and the following arguments), but their appearance does not contain additional informations for the present kind of investigations. To follow the diazotation reaction after every injection (application of 15.3 μmole of NO_2 in 1 ml air in a syringe from a distance of approximately 1 cm) of NO_2 the intensity and distribution of the diffraction signals in α_f were recorded at 4 different angles of incidence and therefore at 4 different penetration depths. The angles of incidence were chosen to monitor the progress of the gas-solid reaction due to the diffraction profiles directly at the surface and at different depths in the crystal bulk. Thereby the values of α_i which are below the critical angle of the total external reflection belong to processes occuring directly at the surface while the measurements at higher angles of incidence describe the propagation of the diazotation within the bulk of the crystal. The angle α_i was set to two values below (0.05 and 0.11°), the value at (0.17°) and one value above the critical angle (0.23°). The depth dependent diffraction profiles were recorded after every addition of NO_2. The integral intensity and the shape of the GID-curve remained unchanged until about 180 μmoles of NO_2 were applied. Continued application

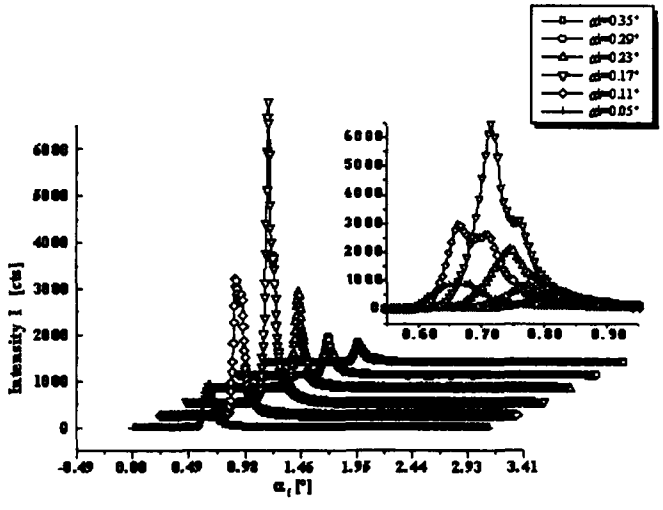

FIGURE 6 Depth dependent diffraction profiles at different angles of incidence α_i at the (002) reflection of the investigated single crystal of 1 before diazotation with NO_2, $\lambda = 1.48$ Å, $2\theta = 24.980°$, $\omega = 56.307°$.

Downloaded by [University of California, San Diego] at 22:15 20 August 2012

of nitrogen dioxide produced a major change in the reaction profiles at an angle of incidence of 0.05°.

A critical value was reached when the integral intensity of the diffraction profile at the surface decreased to one third of the initial intensity within one injection step. Obviously, this critical stage corresponds to the point of phase transformation known from Figure 3d, when the island structures change to irregular aggregates at the surface. A similar interpretation holds for the data obtained at $\alpha_i = 0.11°$ (contour plot in Fig. 7c). Additionally it is observed that the disappearance of the in-plane rocking curve occurs before the decrease of the diffracted intensity which is measured for the (002) reflection of the single crystal. This observation is obviously due to an increasing mosaicity of the crystal prior to significant chemical transformation in that depth range. This process can also be observed at the critical angle of total external reflection (Fig. 8a) with $\alpha_i = \alpha_c = 0.17°$. Thus, an increase in the integral intensity $\int I(\alpha_f)\, d\alpha_f$ continues up to an applied amount of NO_2 of about 180 μmoles while the signal of the in-plane rocking curve has already disappeared. Only in the measurements at $\alpha_i < 0.17°$ continued application of nitrogen dioxide gave rise to an increase of a new signal at $\alpha_f = 0.68°$ which could not be classified yet. Above the critical angle (at $\alpha_i = 0.23°$) the diffracted intensity behaves completely different during the reaction process (Fig. 8b). Within the bulk of the crystal at a penetration depth of up to 0.1 μm the integral intensity $\int I(\alpha_f)\, d\alpha_f$ in the (002) reflection decreases linearly by following the amount of the applied NO_2. From the beginning of the chemical reaction the products are formed according to the formula drawing.

CONCLUSIONS

The experimental results indicate little initial change of the crystal lattice at penetration depths below the critical angle of the external reflection of 0.17°. At low supply of NO_2 reactions at the surface of **1** to give 4-benzenediazoniumsulphonate **3** apply solely to the amino groups of that half of the surface molecules that are freely available on the surface without any need to break hydrogen bonded chains which run down into the crystal bulk. Irregularities which are present on the surface are leveled out (Fig. 2). The integral intensity of the diffraction profiles increases up to a critical transformation with NO_2 and stays nearly constant for the signals at an angle of incidence of 0.05°, i.e. very close to the surface (Fig. 9). The formation of islands with step heights of up to 1.8 nm is in the range of the initial roughness and could not

Downloaded by [University of California, San Diego] at 22:15 20 August 2012

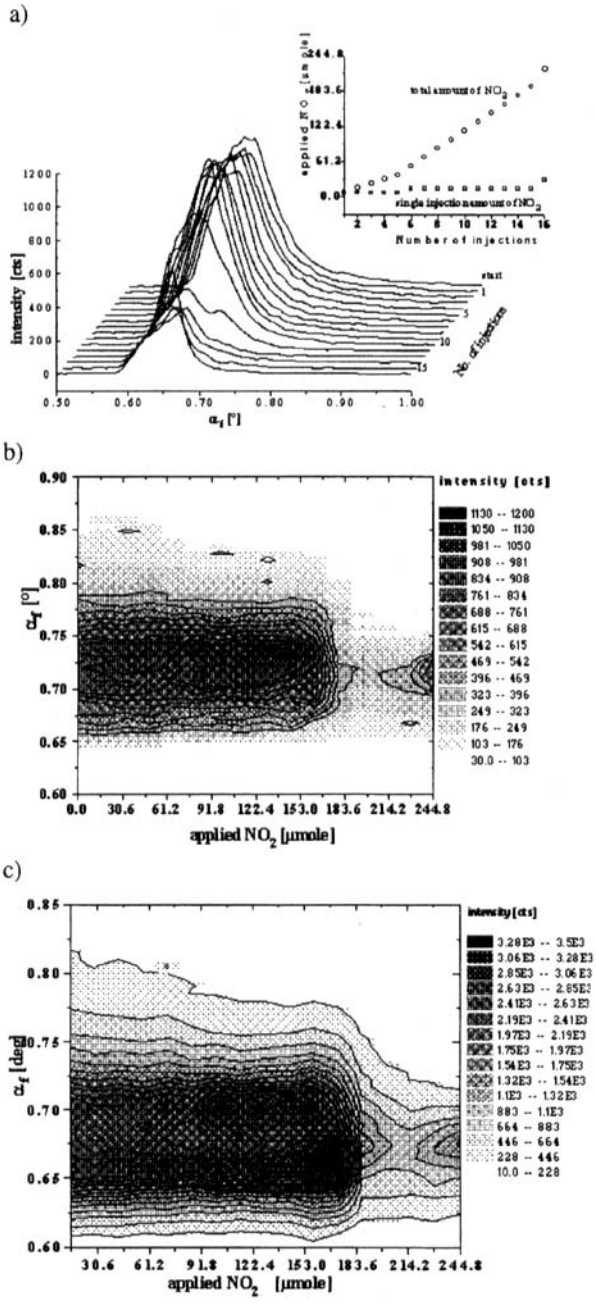

FIGURE 7 Depth dependent reaction profiles of the diazotation of sulfanilic acid monohydrate below the critical angle α_c (a: α_f-profiles with $2\theta = 24.980°$, $\omega = 56.307°$, $\alpha_i = 0.05°$; b: the corresponding grey scale contour plot at $\alpha_i = 0.05°$; c: the contour plot at $\alpha_i = 0.11°$).

Downloaded by [University of California, San Diego] at 22:15 20 August 2012

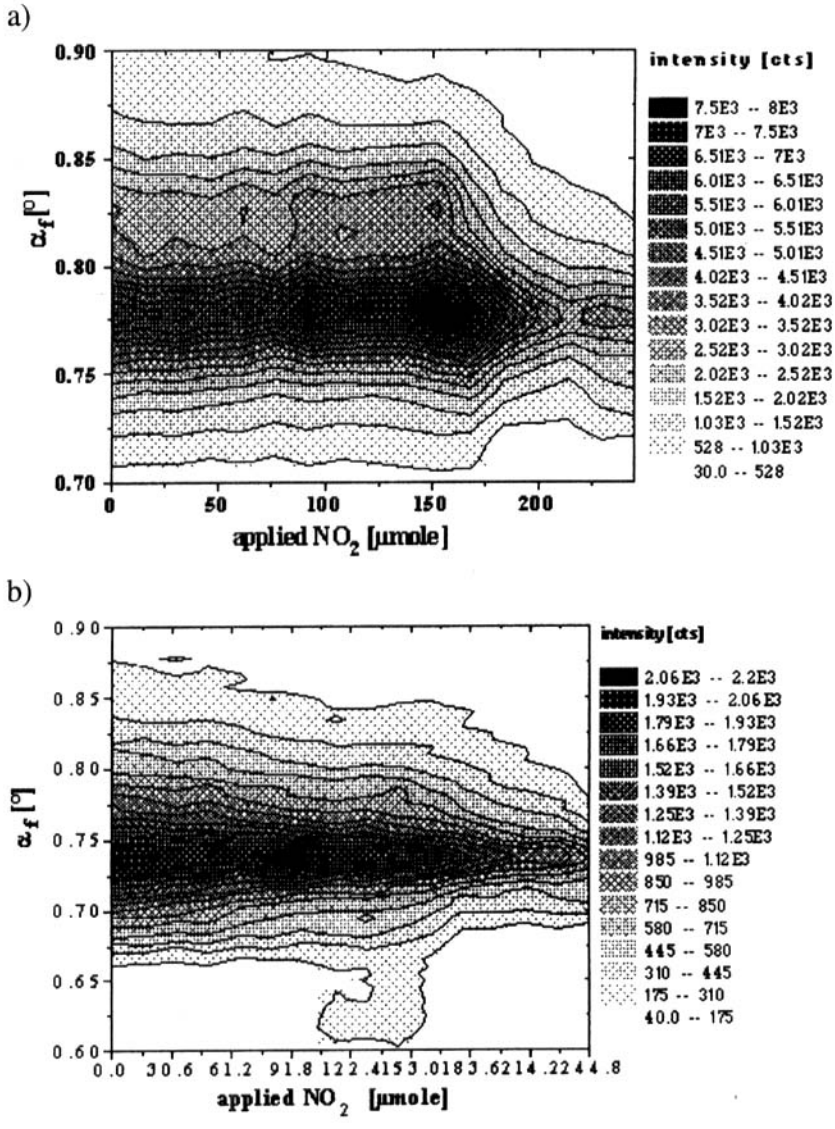

FIGURE 8 Depth profiles; a: at $\alpha_i = \alpha_c = 0.17°$; b: above the critical angle at $\alpha_i = 0.23°$.

be monitored by GID. The data at larger penetration depths indicate the formation of reaction channels presumably along disorder lines or at point defects which appear during chemical reaction and from which the NO_2 gas may efficiently enter into the bulk of the crystal and react with the amino

Downloaded by [University of California, San Diego] at 22:15 20 August 2012

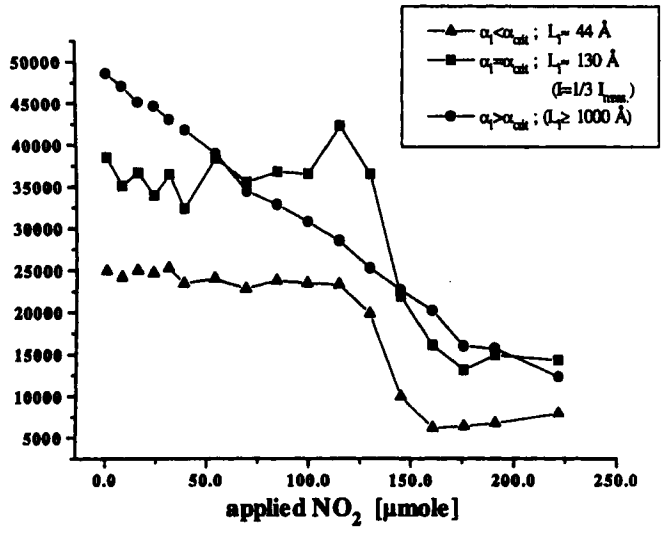

FIGURE 9 Progress of the integral intensities $\int I(\alpha_f)\, d\alpha_f$ as a function of the applied quantity of NO_2 at various angles of incidence.

groups. The crater formation in Figures 1 and 3 are visible signs of that mechanism. Thus, larger regions of the upmost surface remain mostly unchanged, except the rapid reactions of the heads of one half of the molecular chains which are crystallographically inoperative until the reaction from the sides has considerably proceeded. At the critical point of phase transformation, when the initial lattice breaks down and the product lattice forms, the single crystal island structures disintegrate rapidly. That is shown by the sudden decay of the in-plane rocking curve. The polycrystalline domains thus formed (crystallites) open a wealth of new channels for the progress of the diazotation in the crystal bulk. The diffraction signal of the reflex of **1** decreases heavily, the surface disintegrates. The combined consideration of the GID and AFM experiments of the gas-solid diazotation of sulfanilic acid monohydrate **1** provides a sole interpretation. The depth resolved diffractions at grazing incidence show, that besides the initial islands the also formed craters are of particular importance for the reaction. Thus, the combination of surface techniques with the depth resolved in-plane diffraction allows a more comprehensive description of gas-solid reactions in organic crystals, in particular if minute side faces cannot be probed directly by AFM.

Downloaded by [University of California, San Diego] at 22:15 20 August 2012

Acknowledgements

The AFM investigation was supported in part by the Deutsche Forschungsgemeinschaft (DFG). This help is appreciated as well as the financial support by the Bundesminister für Bildung und Forschung (BMBF) under Project No. 055IPAAI8 and HASYLAB under I-95-19. Many thanks are due to Dr. H. Rhan (Hasylab at DESY, Hamburg) for extensive support and continuous advice during the measurements.

Downloaded by [University of California, San Diego] at 22:15 20 August 2012

References

[1] G. Kaupp, *Adv. Photochem.*, **19**, 119 (1995); *Comprehensive Supramolecular Chemistry*, Vol. 8, Chapter 9, Super-microscopy: AFM, SNOM and SXM, Elsevier, Oxford, 1996, p. 381 and references cited therein.
[2] G. Kaupp and J. Schmeyers, *J. Org. Chem.*, **60**, 5494 (1995).
[3] G. Kaupp, J. Schmeyers, M. Haak and A. Herrmann, *LABO-Trend*, **95**, 57 (1995); Engl. translation in WWW under http://kaupp.chemie.uni-oldenburg.de.
[4] A. I. M. Rae and E. N. Maslen, *Acta Cryst.*, **15**, 1285 (1962).
[5] R. L. Sass and J. Lawson, *Acta Cryst.*, **26**, 1187 (1970).
[6] G. Kaupp, *Mol. Cryst. Liq. Cryst.*, **211**, 1 (1992) and references cited therein.
[7] F. Toda, *Reactivity in Molecular Crystals*, Chapter 4, Solid-to-solid organic reactions, Kodansha/VCH, Tokyo/Weinheim, p.177 (1993).
[8] M. D. Cohen, G. M. J. Schmidt and F. I. Sonntag, *J. Chem. Soc.*, 2000 (1964); G. M. J. Schmidt, *ibid.*, 2014 (1964); M. D. Cohen, *Angew. Chem. Int. Ed.*, **14**, 386 (1975); *Mol. Cryst. Liq. Cryst.*, **50**, 1 (1979).
[9] G. Kaupp, M. Haak and F. Toda, *J. Phys. Org. Chem.*, **8**, 545 (1995).
[10] G. Kaupp and J. Schmeyers, *Angew. Chem. Int. Ed.*, **32**, 1587 (1993).
[11] G. Kaupp, J. Schmeyers, M. Haak, T. Marquardt and A. Herrmann, *Mol. Cryst. Liq. Cryst.*, **74**, 315 (1996).
[12] A. Lied, H. Dosch and H. Bilgram, *Phys. Rev. Lett.*, **72**, 3554 (1994).
[13] H. Dosch, L. Mailänder, H. Reichert, J. Peisl and R. L. Johnson, *Phys. Rev.*, **B43**, 13172 (1993).
[14] U. Pietsch, T. H. Metzger and W. Seifert, *J. Appl. Phys.*, **78**, 3144 (1995) and references cited therein.
[15] H. Dosch, *Tracts in Modern Physics*, Vol. **126**, Springer, Berlin, 1992.
[16] A. M. Afanasiev and M. K. Melkonyan, *Acta Cryst.*, **A39**, 203 (1983).
[17] U. Pietsch, W. Seifert, J.-O. Fornell, H. Rhan, T. H. Petzger, S. Rugel and J. Peisl, *Appl. Surf. Sci.*, **54**, 502 (1992).
[18] H. Rhan, *Z. Phys. B*, in press.